EFFICIENCY MEASUREMENT OF MOMENTUM IMBALANCE TRIGGER FOR SUPERSYMMETRY SEARCHES AT CMS AT THE LHC

An Undergraduate Research Scholars Thesis

by

CHRISTOPHER J. DAVIS

Submitted to Honors and Undergraduate Research
Texas A&M University
in partial fulfillment of the requirements for the designation as

UNDERGRADUATE RESEARCH SCHOLAR

Approved by
Research Advisor: David A. Toback

May 2013

Major: Physics

TABLE OF CONTENTS

Page

ABSTRACT

Efficiency Measurement of Momentum Imbalance Trigger for Supersymmetry Searches at CMS at the LHC. (May 2013)

Christopher J. Davis
Department of Physics and Astronomy
Texas A&M University

Research Advisor: Dr. David A. Toback
Department of Physics and Astronomy

In searches for new fundamental particles in high energy particle collisions, the ability for a detector to select collisions that might signify the presence of such particles is one of the top priorities. Equally important is to determine how well the selection is done so that procedures can be used to optimize the selection. One such method of collision event selection is known as the momentum imbalance trigger at the CMS detector at the LHC for use in a search for new particles from an extension of the standard model, known as supersymmetry. In this thesis, we describe this trigger and how is it used for searches. Also, we measure the efficiency of the trigger in general operations as well as the impact the number of collisions that occur at the same time has on its performance.

ACKNOWLEDGMENTS

This research was supported, in part, by funds from Texas A&M Honors and Undergraduate Research, the A&M department of Physics and Astronomy, and also the Norman Hackerman Advanced Research Program. Also, I would like to thank the Brazos cluster at A&M which I used extensively in my research. Finally, I would like to acknowledge Will Flanagan, Dr. Alfredo Gurrola, and Dr. Teruki Kamon for their help with this project and my advisor Dr. David Toback for his guidance and support for this thesis.

CHAPTER I

INTRODUCTION

Theory

Standard Model

The current and best explanation of particles and their interactions is described in the theory known as the Standard Model of particle physics (SM) [1]. This theory has been able to predict new particles, and its final predicted particle, the Higgs Boson, is was recently discovered at the Large Hadron Collider (LHC) [2]. Fundamental SM particles are divided into two main categories: fermions and bosons. Fermions have half-integer spin and are divided into quarks (q) and leptons (l). Bosons have integer spin and are the Higgs Boson and the gauge mediator particles. These gauge mediator particles mediate three of the main forces in nature: the W and Z bosons mediate the weak nuclear force, the gluon mediates the strong nuclear force, and the photon mediates the electroweak force. Despite its successes, the Standard Model is not a complete theory. One piece of convincing evidence for new physics beyond the Standard Model is the observation that only 5% of the energy in the universe is from SM particles [3] and that 23% of the energy in the universe is a type of matter, called dark matter, that the Standard Model cannot describe. These dark matter particles do not interact electromagnetically and are only indirectly observable due to their gravitational effects.

Supersymmetry

The leading theory that addresses many of the issues with the SM and also provides a possible candidate to be dark matter is called supersymmetry (SUSY) [4]. This theory is

an extension of the SM and predicts the addition of a new set of particles that are related to their SM counterparts. Every bosonic SM particle has a fermionic SUSY counterpart and vice-versa. The SM quarks (q) and leptons (l) have SUSY partners called squarks ($\tilde{q}$) and sleptons ($\tilde{l}$), where SUSY partners are denoted with a tilde. The SUSY partners of the SM Higgs and gauge mediators are mixed states depending on their charge and form mass eigenstates that are called charginos ($\tilde{\chi}_1^{\pm}$, $\tilde{\chi}_2^{\pm}$) and neutralinos ($\tilde{\chi}_1^0$, $\tilde{\chi}_2^0$, $\tilde{\chi}_3^0$, $\tilde{\chi}_4^0$). A conserved quantity called R-parity prevents SUSY particles from decaying into only SM particles as SUSY particles have R-parity of -1 and SM particles have R-parity of $+1$ [5]. This causes the lightest SUSY particle (LSP) to be stable and to be a valid dark matter candidate if neutral.

Coannihilation

Supersymmetry is a broken symmetry since the masses of SM particles are not the same as their massive SUSY counterparts. One possible proposed mechanism for this breaking is called minimal super gravity (mSUGRA) [4,6]. The most general models of SUSY have 128 free parameters, but models of mSUGRA are well definied by 5 different parameters. One of the most important regions of the parameter space is known as the $\tilde{\tau}_1$-$\tilde{\chi}_1^0$ coannihilation region [7]. In the coannihilation region, the $\tilde{\chi}_1^0$ is the LSP, the $\tilde{\tau}_1$ and the LSP have similar masses. This is important because the similar masses would give them similar densities in the early universe and annihilation between them into SM particles is an important determination of the amount of dark matter that exists today [8]. One of the advantages of coannihilation is that it can be used to explain the observed dark matter density from experiments such as the WMAP experiment [3]. If this model correctly describes nature, then when high-energy protons are collided at the LHC, SUSY particles should be produced and decay, leaving a specific signal in the detectors. An example of the production and decay of such a scenario is shown in Fig.I.1.

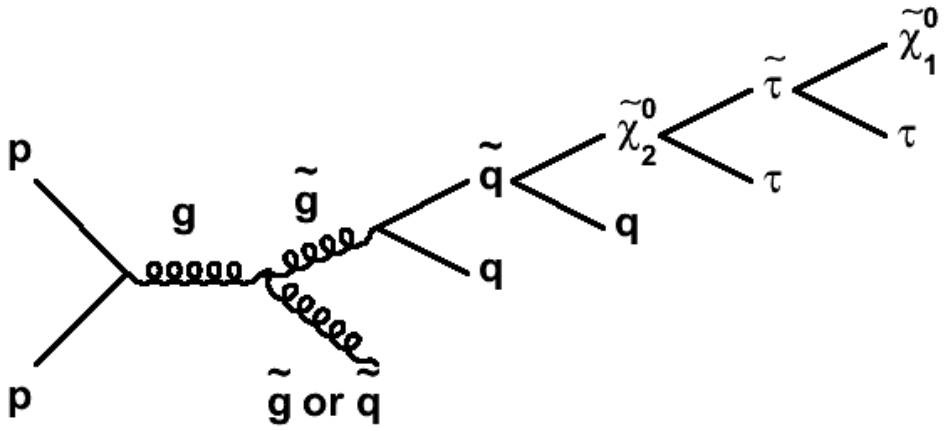

Fig. I.1. This is a diagram showing how an event producing SUSY particles would occur at the LHC according to the parameters of the coannihilation region. The two protons on the left interact and form a characteristic final state of quarks (q), taus (τ), and a neutralino ($\tilde{\chi}_1^0$).

Phenomenology

Sparticle Production at the LHC

When two SM particles such as protons collide at very high energy, there is a possibility for new particles to created. If there are SUSY particles in nature with the right masses and couplings, then these particles can be produced in these collisions. The particles produced are generally very short-lived and do not travel any appreciable distance before they decay. Therefore, the particles that can be detected and measured are the particles that live long enough to actually interact with the detector itself. The particles that are observed in (or travel through) the detector are called the final state particles.

Methods of Observing New Physics at the CMS Detector: Final States

A characteristic signature of many SUSY models is the $\tilde{\chi}_1^0$ in the final state. All the particles in the final state, except for the $\tilde{\chi}_1^0$, will leave tracks in the detector and deposit all of

their energy. The $\tilde{\chi}_1^0$ will neither leave tracks, nor deposit any energy in the detector. This causes any reconstruction of the event to have momentum imbalance since the $\tilde{\chi}_1^0$ that would have balanced the event is not detected. Missing transverse momentum (MET) is a general signature of SUSY as shown in Fig.I.2 as events with large values of MET can, in principle, be used to separate events from SM and SUSY origins. This allows for the extra SUSY events to be noticeable against the small background of SM events.

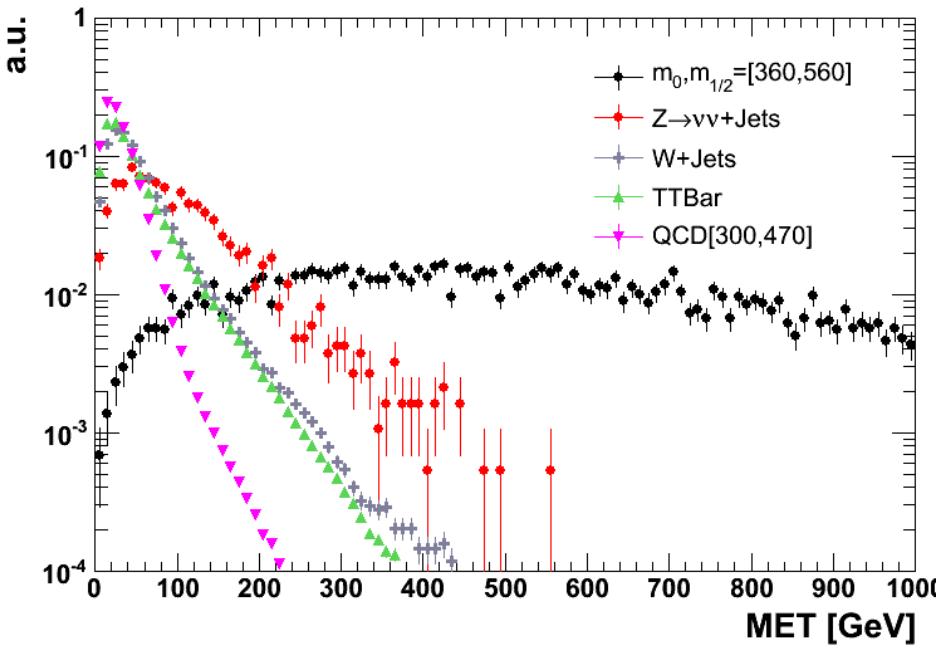

Fig. I.2. The distribution of MET for events from various SM sources along with an example source of SUSY events. At low MET, SM events are the majority, but, at high MET, SUSY events are the majority. This shows that selecting events with large values of MET can separate SM and SUSY events.

We note that one of the primary goals of the research program and, if successful, which version of SUSY is correct. One of the features that distinguishes between the coannihilation region version and other versions is in the decay of the second lightest neutralino, $\tilde{\chi}_2^0$ which decays via: $\tilde{\chi}_2^0 \rightarrow \tau\tilde{\tau}_1 \rightarrow \tau\tau\tilde{\chi}_1^0$ [9]. In a sophisticated search for SUSY, events with taus can be identified and indicate which version of SUSY is correct in nature and also if the

coannihilation region explanation of the dark matter density is correct. This specific signature is unique as there are very few SM processes which have 2 taus and missing transverse momentum. However, colliders such as the LHC that create taus in high-energy collisions undergo billions of collisions per second, and all of these collisions are quickly analyzed for the presence of MET and analyzed offline for the presence of taus.

In the experimental design, there are many millions of events that must be studied per second. To select the small number of interesting events in real time, we use what is known as a trigger. These triggers will either pass or reject events in real time based on whether or not a trigger requirement is fulfilled (for example, if it has large MET). If the event passes all the requirements, then the event is written to disk. If not, the trigger will simply move on to consider the next event. However, before we can study events that passed the trigger system in a full systematic way, we need to study how well the trigger system works.

Our experimental apparatus, which studies high energy proton-proton collisions created by the Large Hadron Collider (LHC), is a multi-purpose detector known as the Compact Muoun Solenoid (CMS). The trigger we use at CMS is a momentum imbalance trigger. This trigger is especially useful for SUSY particle searches in general because it will record any event that has high MET. This thesis focuses on how well this trigger responds to the presence of events that occur in our detector using various methodologies and see how well it records these types of events.

Overview of the Thesis

This thesis is part of a large effort to search for SUSY in the coannihilation region at CMS. A typical search of this nature is done is a group with a graduate student, a post-doc, and a faculty advisor, and typically takes a full graduate school career. The search itself includes the data taking process to select events with large MET in real time with the triggers and then a selection of the subset of events with two taus for a comparison of the results to the

SM-only hypothesis and the SUSY hypothesis. My role was to work on a fundamental issue in the search to determine if the CMS detector is sensitive enough to be able to even detect events with the signature we are searching for and, if the detector is sensitive, how well the detector is working. In terms of the final state, my work was to determine how well the MET trigger can record events with high MET, while others worked to find taus and do the final analysis. The final search, with the taus and comparison to expectations, will be completed by my colleagues, but, in this thesis, I will present my contribution to the analysis effort. For this reason, Chapter 1 describes the big picture of the analysis in order to understand the context of my efforts.

Chapter 2 begins by describing the experimental apparatus of the LHC itself and then moves to discuss the CMS detector located in the LHC. It will explain what occurs when particles collide in the CMS detector and how the CMS detector is designed to detect and measure these particles. It also describes how the CMS detector uses a trigger system to record important events with an emphasis on the momentum imbalance trigger. Chapter 3 describes the measurement of the efficiency of the momentum imbalance trigger at CMS and how it is affected by the number of hard-scattering events in the detector. Chapter 4 summarizes the results from my successful efforts studying the MET trigger and measuring its response and usefulness, discusses possible improvements to the results from the trigger study, and describes how this analysis will be concluded for the final search for SUSY in the coannihilation region.

CHAPTER II

THE LARGE HADRON COLLIDER

The LHC is a particle accelerator built by the European Center for Nuclear Research (CERN) beneath Geneva, Switzerland and is a circular structure, spanning 27 km in circumference, crossing the border between France and Switzerland. The LHC is located at an approximate average of 100 meters underground, and the main accelerator is comprised of 1232 dipole magnets, allowing for, in 2012, $\sqrt{s} = 8$ TeV center-of-mass energy for two colliding proton beams, one traveling clockwise, the other anticlockwise [10]. During the 2012 runs of the LHC, which is the dataset for this study, these protons were arranged so that collisions occur every 50 nanoseconds. These proton bunches are collided into each other at the center of the detectors.

A quantitative measure of the number of protons in a bunch and their density is given by the luminosity of the LHC. The instantaneous luminosity is the number of interactions per unit area per unit time, and the integrated luminosity is the luminosity integrated over a certain time, such as over a run, and is given in units of barns. A barn, b, is a unit of area where $1\ b = 10^{-24}\ cm^2$. The luminosity is given by this formula:

$$L = \frac{N_b^2 n_b f \gamma_r}{4\pi\epsilon_n \beta^*} F \tag{II.1}$$

where N_b is the number of particles per bunch, n_b is the number of bunches per beam, f is the frequency of revolution, γ_r is the relativistic factor for particles traveling at velocities near the speed of light, ϵ_n is the transverse beam emittance, β^* is the betatron function at the collision point, and F is the reduction factor due to the crossing angle. The design instantaneous luminosity of the LHC is $10^{34}\ cm^{-2}\ s^{-1}$ or $10\ nb\ s^{-1}$. This luminosity produces about 15 proton-proton collisions per bunch crossing.

The expected number of events produced in a process is related to the integrated luminosity, L, by this formula:

$$N = L \cdot \sigma \tag{II.2}$$

where σ is the production cross section of the event in units of area. The cross section can be thought of as the size of the target for the process, for example from SUSY, that the beams are hitting whenever proton bunches collide. In this thesis, we make use of 5.75 fb^{-1} of $\sqrt{s} = 8$ TeV pp collision data of Run2012 A and B data collected by the CMS detector between April and December 2012. If the SUSY production cross section were 100 fb, we would expect roughly 575 events to be produced in addition to the SM backgrounds.

Compact Muon Solenoid Detector Overview

One of the two largest detectors at the LHC is the CMS detector. This detector is designed to be able to be sensitive to the kinds of signals expected from SUSY events, with its layout shown in Fig. II.1.

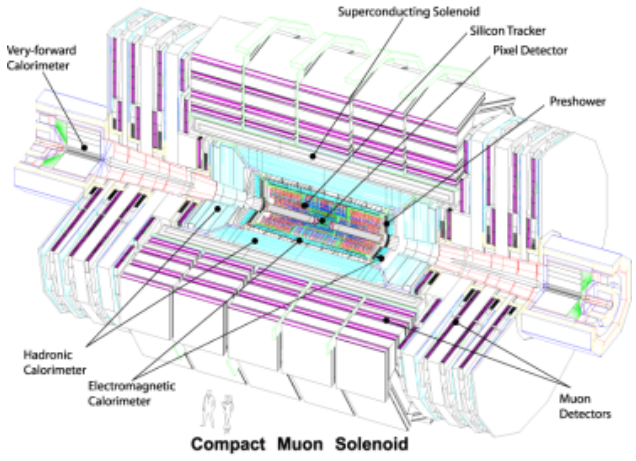

Fig. II.1. A view of the CMS detector at the LHC.

The detector is 13 meters long and contains a 5.9 meter inner diameter superconducting solenoid producing a 4 Tesla magnetic field. This large magnetic field allows for the measurement of the charge and momentum of fast-moving charged particles as they experience a Lorentz force while traveling through the detector. The coordinate system of the detector is defined where the x-axis points towards the center of the ring, the y-axis points vertically upwards, and the z-axis points along the beam direction. The azimuthal angle ϕ is measured from the x-axis in the x-y plane. The angle θ is measured from the z-axis. Another quantity called pseudorapidity is used more often than θ and is defined by the equation

$$\eta = -\ln(\tan\frac{\theta}{2}). \tag{II.3}$$

The quantity of pseudorapidity, η, is generally more useful than θ since η is invariant under a relativistic transformation along the z-axis. Using η also allows for a useful description of how many particles are incident in a region since most pp collisions at the LHC are deflections where the resulting particles are more likely to hit the more forward regions, the endcaps of the detector, than the middle regions, the barrel of the detector. As a reference, the region in Fig. II.2 from $\eta = 0$ to $\eta = 1$ will see approximately as many particles as the region from $\eta = 2$ to $\eta = 3$.

At design center-of-mass energy ($\sqrt{s} = 14$ TeV), luminosity, and bunch spacing (25 ns), the CMS detector will observe an event rate of approximately 10^9 inelastic events per second. This many events cannot possibly all be recorded each second, so an online selection process (trigger system) was implemented to reduce the billion interactions per second down to about 100 events per second selected to be stored for later analysis. Further complicating this process, 16 additional collisions will also occur in the same bunch, on average, as any interesting event at design luminosity. This trigger system has to be robust enough to handle processing of events every 25 ns, yet still be able to perform correct reconstruction of multiple events from approximately 1000 charged particles in each event. The way this is achieved is through fast hardware-based Level-1 (L1) trigger system, and a slower but more powerful

software-based High-Level Trigger (HLT) system. The L1 system is used to quickly accept or throw out events so that no more than 10^5 of the stored events are sent to the HLT system which trims down the events to the final 100 events per second that is saved for analysis. A full description of all the L1 and HLT triggers is too long for this thesis, but is available at [10, 11]. The parts of the detector that are used by the trigger systems are in Fig. II.2 and we briefly describe each.

Measuring Momentum at CMS

Since the important quantity for this study is the missing momentum of the final state particles, it is important to discuss how the momentum of a particle is measured in different parts of the detector as it travels outwards from the center of the CMS detector.

Tracker

The tracker is used to reconstruct the paths that the charged particles, namely muons, electrons, and charged hadrons, that were created as products of the collision as they traverse from the collision position radially outward. Each location in the tracker where a charged particle is detected is known as a "hit". The hits, in turn, can be used to reconstruct the full trajectory and 4-momentum of each of the charged particles which can be combined to determine the position of each of the collision events, known as a vertex, and will be described later. The tracker system is made of silicon pixel detectors closest to the center ($11 <$ r < 20 cm). The size of a pixel in x- and y-coordinates is $\approx$ 100 x 150 μm^2. In the middle of the tracker ($20 < r < 55$ cm), the tracker system consists of silicon microstrip detectors with a minimum cell size of 10 x 80 μm^2. In the outer region (55 cm $<$ r $<$ 115 cm), larger silicon microstrips are used with a maximum cell size of 25 cm x 180 μm.

Calorimeters

When a charged particle travels through the tracker, it only deposits a small fraction of its energy while interacting with the detector while neutral particles do not interact. However, in the calorimeters, nearly all of the energy of the particles is deposited and measured. The calorimeters are segmented into two types of detectors: The electromagnetic calorimeters and the hadronic calorimeters.

Electromagnetic Calorimeter

The electromagnetic calorimeters (ECAL) are located outside the tracker and are used to identify photons and electrons and measure their momentum. The barrel ECAL is made of avalanche photodiodes with an active lateral area of $5x5mm^2$ each that are attached to crystals arranged in $5x5$ units. The crystal radial length is 230 mm which corresponds to 25.8 X_0, where X_0 is the length over which an electron loses all but e^{-1} of its energy due to a process called Bremsstrahlung. Charged particles will deposit energy through this process when they slow down by emitting "braking" photons which are collected in the ECAL. The ECAL at CMS has very good energy resolution of order $3\%/\sqrt{E}$.

Hadronic Calorimeter

Similar to the ECAL, the hadronic calorimeters (HCAL) located outside of the ECAL are used to do the same measurement for the decay products of quarks or gluons (collectively called jets). The HCAL at CMS is a sandwich detector made up of two main parts: a steel and lead absorber to break apart particles and also scintillators to collect light from the showers. The way that neutral hadrons such as neutral pions or kaons (different arrangements of quarks that are commonly produced at the LHC) are detected is to have them break apart into charged particles when they interact with the steel and lead nuclei in the calorimeter

and then measure the energy of the shower of particles that result. The HCAL has an energy resolution of order $40\%/\sqrt{E}$.

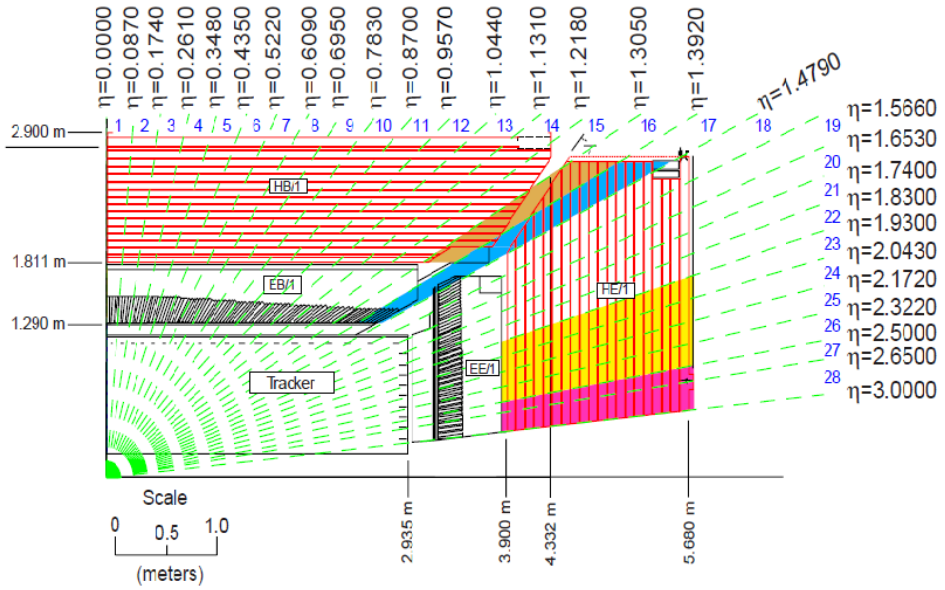

Fig. II.2. A view of the calorimeters and tracker in the CMS detector. The tracker is the closest to the center, followed by the ECAL in the barrel (EB) and endcap (EE), and then the HCAL in the barrel (HB) and endcap (HE).

Particle Flow

Because the tracker has a much higher resolution than the HCAL, an algorithm at CMS was developed to accurately measure the energy of jets that are also detected in the tracker. This method allows for the energy of charged jets to be measured in the tracker instead of the HCAL and only causes neutral hadrons to have their energy calculated in the HCAL. This method of using the tracker to help measure the energy of charged hadrons instead of only relying on the HCAL alone allows for a more accurate measurement of the momentum.

Tracking and Event Reconstruction

Track Reconstruction

Tracks used in the jet measurement and vertexing are reconstructed in 5 stages: hit reconstruction, seed generation, pattern recognition or trajectory building, ambiguity resolution, and a final track fit. Groupings of hits called clusters are reconstructed by searching for tracker microstrips with a signal to noise ratio S/N > 3 and nearby microstrips are included if they satisfy S/N > 2. These clusters are used to recreate the path of a particle and each reconstructed path starts at a cluster called a seed. Three hits are used to start trajectory building. Trajectories are built according to a combinatorial Kalman filter method that proceeds iteratively from the seed layer outwards, adding more precision with the information from each layer [10]. Finally, ambiguities in the track trajectories need to be resolved when a track may be reconstructed from different seeds or because a seed may result in multiple trajectory candidates. To avoid double counting of tracks, the ambiguities are resolved based on the fraction of hits shared between the 2 trajectories, or, if the fractions are equal, the track with the highest χ^2 value is discarded. The ambiguity resolution is applied twice: on all tracks from a single seed, and all track candidates from all seeds. At the end of the tracking procedure, we are left with a set of unique tracks.

Vertex Reconstruction

Using reconstructed tracks that intersect at the beam line allows for a measurement of all the primary vertices and a precise measurement of each vertex position. A primary vertex occurs from a pp collision along the beam line, whereas secondary vertices occur off the beam line when produced particles decay. An example event showing the trajectories of multiple charged particles and the reconstructed vertices is shown in Fig. II.3.

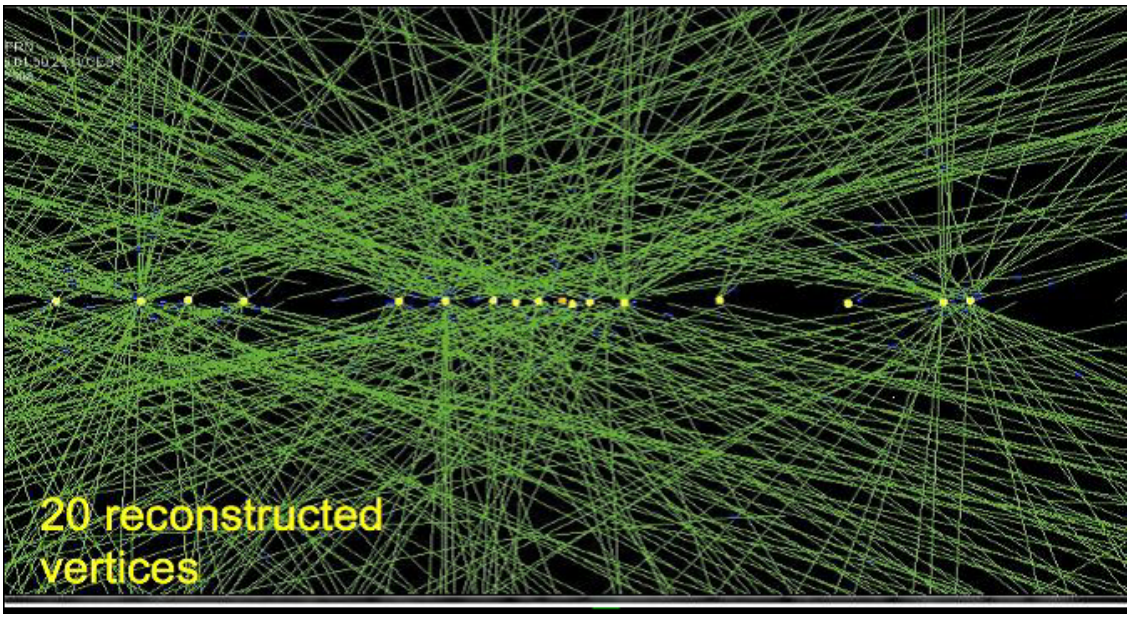

Fig. II.3. Reconstructed tracks and vertices from a sample event in the CMS detector, shown in a cross-sectional view with the x-axis corresponding to the z-axis of the detector and the y-axis along a radial direction on the barrel. The large yellow dots are the primary vertices and are aligned along the z-axis of the detector.

As evident in the figure, there are often many primary collisions in each event that are reconstructed as primary vertices. A measurement of the reconstructed number of primary vertices is known as a "pile-up". As we will show, the number of pile-up interactions can significantly affect the measurement of important quantities such as the momentum imbalance.

Missing Energy and Missing Energy Triggers

MET

The momentum of the resulting particles that are produced by the collisions are measured in the tracker, ECAL, HCAL, and muon detectors. The detector itself cannot cover the entire solid angle of the detector itself, but the transverse momentum, $\vec{p_T} = \vec{p}\sin(\theta)$, can be

measured to high accuracy because the area perpendicular to the events are well-covered by the detectors. The vector sum of the transverse momentum forms a useful quantity called MET which is the momentum imbalance. MET is defined by the equation

$$\vec{MET} = -(\sum_{jets} \vec{p_T} + \sum_{photons} \vec{p_T} + \sum_{leptons} \vec{p_T}). \tag{II.4}$$

MET also has a scalar form given by

$$MET = |\vec{MET}|, \tag{II.5}$$

and, for the purposes of this thesis, we will use the term MET to refer to this scalar form, i.e., the magnitude of the MET. In a perfect detector where all the particles were detected, by conservation of momentum, the vector MET would be identically zero. However, if a particle, such as a $\tilde{\chi}_1^0$, leaves the detector without interacting, it will not contribute to the vector sum of the MET and can cause the measured value of the MET to be significantly different than zero as shown in Fig. I.2.

MET Triggers

The MET triggers at CMS calculate the MET for any events that are passed to them from the L1 triggers. When an event occurs where the MET is higher than some threshold value, the event is recorded for use in later analysis. However, the presence of pile-up collisions degrades the measurement of MET, as transverse momentum from a second collision could cause the trigger to pass events where the MET from the main collision is less than the threshold value or cause the trigger to not pass events where the MET is higher than the threshold value.

However, MET cannot be measured with complete accuracy at speeds on the order of the collision spacing at the LHC. On these timescales, the L1 trigger only has time to consider

coarse momentum measurements from the calorimeters, but the High-Level trigger does have more time to use information from the tracker and the outer muon detectors to make a more accurate measurement of MET which is also improved by using Particle Flow. If the trigger worked perfectly, then every event where MET were measured to be higher than 150 GeV would also pass the MET trigger, and every event where MET were measured to be lower than 150 GeV would not pass the trigger. Even with Particle Flow algorithms, the trigger is imperfect which causes some events with more than 150 GeV of energy to not pass the trigger and some events with less than 150 GeV of energy to pass the trigger. Events with low MET are unlikely to pass the trigger, and events with high MET are unlikely to not pass. For events with MET close to 150 GeV, small mis-measurements can cause the trigger to give an incorrect reading.

The MET trigger studied in this analysis is known as the HLT_PFMet150 trigger which passes events that have MET higher than 150 GeV and rejects events with less than 150 GeV MET. HLT stands for High-Level trigger which means that this trigger is done at the last stage of the CMS trigger system. PF stands for Particle Flow which, as mentioned earlier, allows for a reliable measurement of the momentum of outgoing particles from the detector.

MHT

A useful quantity that we use to identify SUSY events is known as MHT, defined by the equation

$$MHT = |\sum_{photons} \vec{p_T} + \sum_{electrons} \vec{p_T} + \sum_{taus} \vec{p_T} + \sum_{jets} \vec{p_T}|, \text{ where } |\vec{p_T}| > 30\,\text{GeV}. \tag{II.6}$$

In particular, we do not consider all the energy in the detector from each collision, instead we only consider high energy objects which are most likely from a primary collision. If a SUSY

event were produced, it is very likely that all the high energy objects would be from only that collision. Thus we consider only objects with a $p_T > 30$ GeV. One of the advantages of MHT is that it has a p_T threshold for the values that it uses in its calculation. If a particle deposits less than 30 GeV in the detector, it isn't registered in MHT. Pile-up events will generally emit particles that have low p_T, so MHT will be less influenced by various values of pile-up. However, MET will take the p_T from these events in the calculation. This makes MHT attractive as a quantity to use in analysis because MHT will have less dependence on pile-up than MET. It is then important to measure how the MET triggers pass events that have various amounts of MHT. It will make analysis easier if the MET triggers are independent of MHT after some value of MHT. Therefore, we measure the efficiency of the MET triggers as a function of MHT in the next chapter.

CHAPTER III

MOMENTUM IMBALANCE TRIGGER STUDY

Method

The momentum imbalance trigger was used throughout the data taking and we now wish to measure its efficiency. The efficiency for a trigger is given by the number of events that pass the threshold of the trigger divided by the total number of events seen by the trigger, or

$$\epsilon = \frac{N_{pass}}{N_{total}}. \tag{III.1}$$

For each event, the trigger will compare the quantities in the event to the trigger requirements and give either a "pass" or a "fail" answer.

We cannot measure the efficiency of the trigger by considering all the events observed by the trigger as data. The difficulty in measuring the efficiency with real data arises in determining the total number of events which must be considered in the denominator, however. We cannot measure the efficiency of the trigger by considering all events observed by the trigger as data because not all events considered by the trigger are written out for further consideration. For this reason, to measure the efficiency of the trigger we must use events that were selected by the trigger system but are selected by a separate trigger that is independent of the MET trigger. To understand this we note that if a dataset is used where most of the events have passed another trigger that is correlated with a MET trigger, then using such a sample to estimate the efficiency would yield a biased value. In particular, the efficiency would be much higher than the actual efficiency.

To minimize this problem, we use a set of data that passes a second trigger that is entirely uncorrelated with MET but also has a large variety of values of MHT. This allows us to see how the efficiency changes as a function of MHT. The efficiency of the uncorrelated trigger

is not important since that would only affect the number of events in the dataset and not the measured efficiency of the MET trigger itself. The dataset used for this analysis was CMS data where a single muon (a type of lepton which is similar to an electron, but more massive) was recorded by the CMS detector system. The CMS detector does not have a bias for detecting a single muon depending on MET, so this dataset was used in the analysis.

Results

The sample of events with a single muon is used as a way of measuring the trigger efficiency by considering the fraction of events which have a muon and pass the momentum imbalance trigger divided by the total number of single muon events. Using the single muon sample events, we measure the trigger efficiency as a function of MHT. Specifically, for every event we measure the MHT and consider this a denominator event. If it passes the momentum imbalance trigger then it is a numerator event. The fraction of events passing the trigger as a function of MHT is shown in Fig. III.1.

As expected, the efficiency starts at zero and increases rapidly at high MHT, eventually plateauing well above the trigger threshold. Since it is useful to have a parameterization of the trigger efficiency as a function of MHT, we fit to an error function of the form

$$Eff(MHT) = C_0 * \frac{1}{2} * erf((MHT - C_1) * \frac{1}{2 * [C_2]} + 1) \tag{III.2}$$

where the parameter C_0 is the plateau, C_1 is the threshold MHT value where the efficiency reaches 50%, and C_2 is the width of the curve in MHT. The best fit values are listed in row 1 of Table III.1. Of particular importance is that well above the threshold of 150 GeV we have 95% efficiency which is quite useful for searches for SUSY as shown in Fig. I.2.

While this efficiency is important, it is no less important to see how the trigger efficiency is affected by pile-up. A large number of collisions in a single event could degrade the resolution

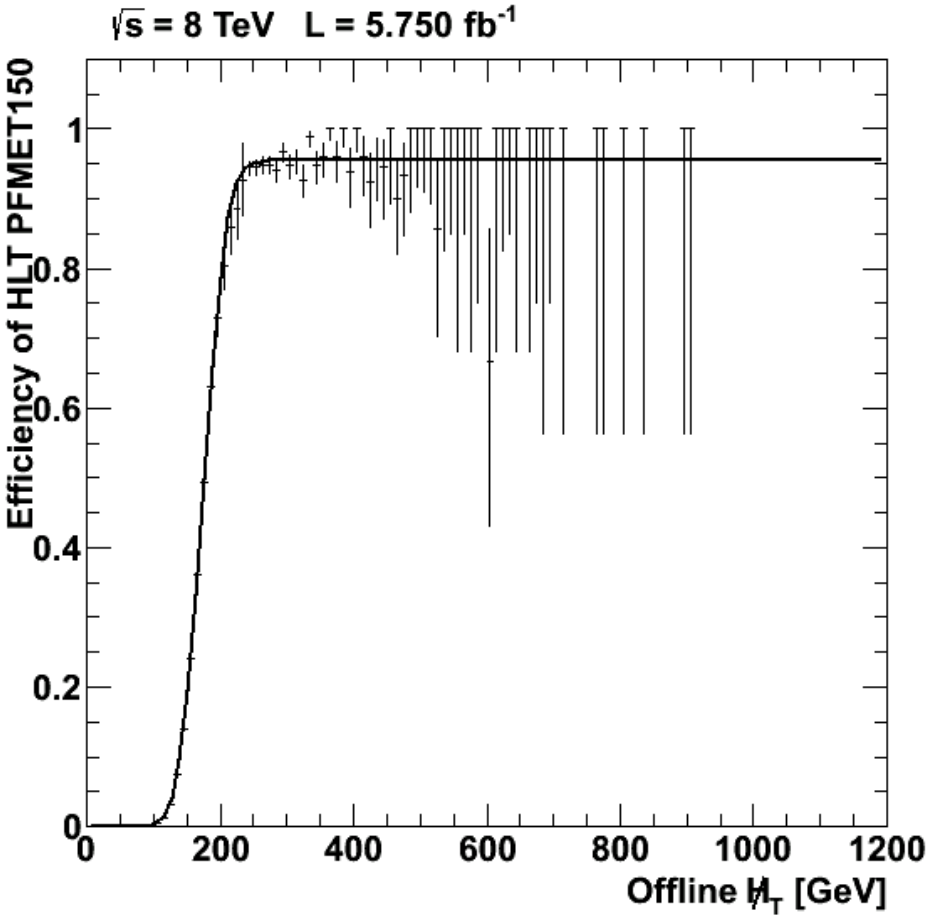

Fig. III.1. The efficiency of the HLT_PFMet150 trigger as a function of offline MHT (symbolized with a $\not{H}_T$).

of the MET or otherwise cause a reduction in the trigger efficiency. If the number of primary vertices causes a change in the efficiency, then there would be a dependence on the amount of pile-up for the efficiency, which would cause a lot of difficulty for any later analysis using this trigger.

Pile-up Effects

To study the effects of pile-up, the events in the dataset is broken up into three subsamples depending on how many primary vertices there are observed. A histogram of the number of events as a function of the number of vertices is shown in Fig. III.2. For simplicity, the dataset is divided into three regions:

1. low pile-up (Nvertices < 8)
2. average pile-up ($8 \leq$ Nvertices ≤ 20)
3. high pile-up (NVertices > 20)

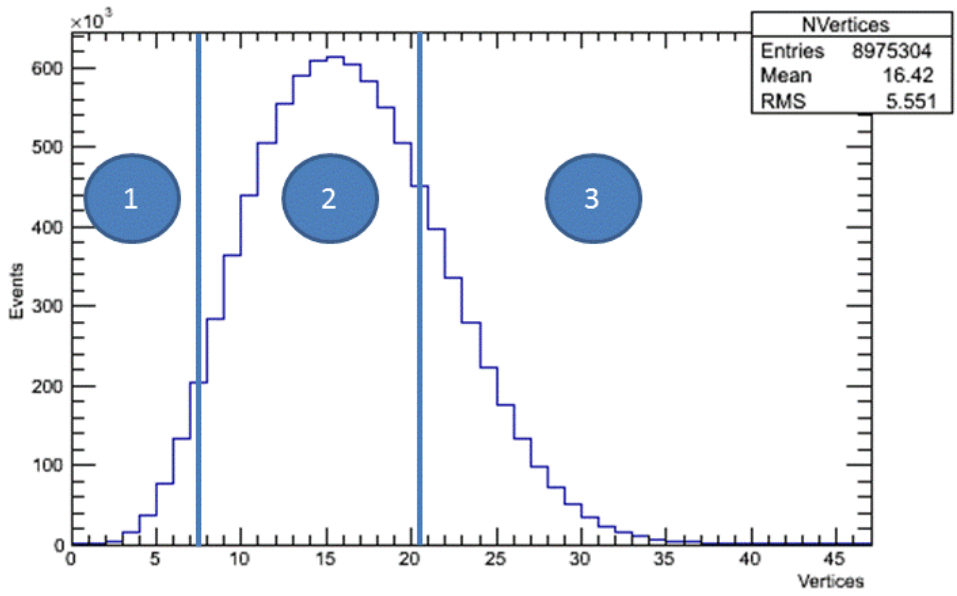

Fig. III.2. Histogram showing the number of events per number of reconstructed vertices. Where each of the regions are is shown.

Each of these regions can be treated as a different dataset and run through the same procedure as for the original, complete dataset. The measured fit parameters from Equation III.2 are listed in Table III.1 along with the parameters for the full sample. The plateau efficiency is plotted as a function of the number of vertices in Fig. III.3

NVertices	Efficiency Plateau	Threshold (GeV)	Width (GeV)
All Data	95.5 ± 0.4%	174.3 ± 0.4	19.4 ± 0.2
Nvertices < 8	94.8 ± 1.0%	168.3 ± 1.0	15.2 ± 0.6
8 ≤ NVertices ≤ 20	95.8 ± 0.4%	174.1 ± 0.5	19.2 ± 0.2
NVertices > 20	93.4 ± 1.0%	175.3 ± 1.0	20.5 ± 0.4

Table III.1

Fit parameters of each region. Note that all of the errors are statistical errors only. The larger errors are due to lower statistics in the high and low pile-up regions. However, we note that the parameters show small variation and are basically consistent with the observed statistical uncertainties

Since the important region for analysis is in the high MHT region, another way to look at the data is to look at how pile-up just affects the plateau efficiency in the high MHT region. To do this,we just do a linear fit in the plateau region where the efficiency levels off, i.e., where MHT > 250 GeV. The linear plateau region efficiency vs. the number of reconstructed vertices (NVertices) is shown in Fig. III.4. A comparison between the two methods is shown given in Table III.2

NVertices	Linear Efficiency	Efficiency Plateau
NVertices < 8	97.5 ± 1.6%	94.8 ± 1.0%
8 ≤ NVertices ≤ 20	96.9 ± 0.4%	95.8 ± 0.4%
NVertices > 20	95.7 ± 1.0%	93.4 ± 1.0%

Table III.2

Comparison of the Linear measurement of the efficiency and the measured efficiency plateau for various levels of pile-up.

Although there are larger statistical errors in the first and last bins, there is the worrisome indication that more primary vertices cause a decrease in efficiency. Although the trigger is able to pass over 95% of the events in the plateau region, the pile-up effects could be problematic for any analysis using the trigger.

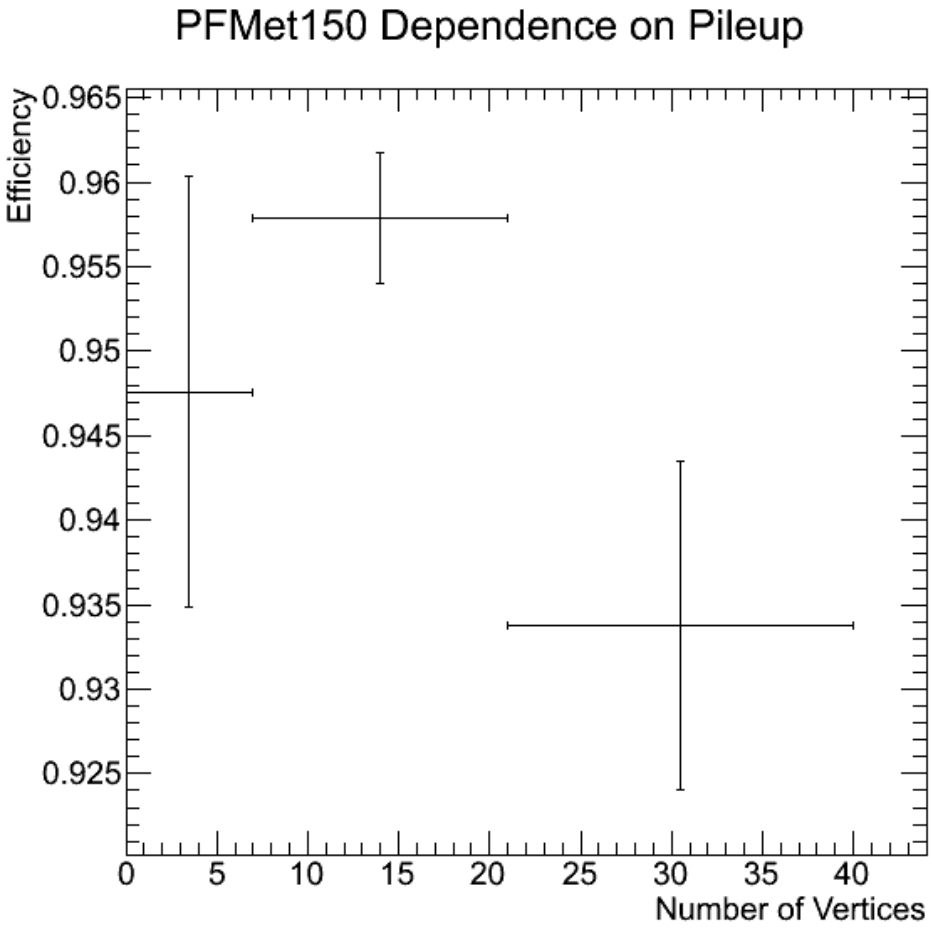

Fig. III.3. The measurement of the plateau efficiency using the full parametrized efficiency fit for different regions of pile-up.

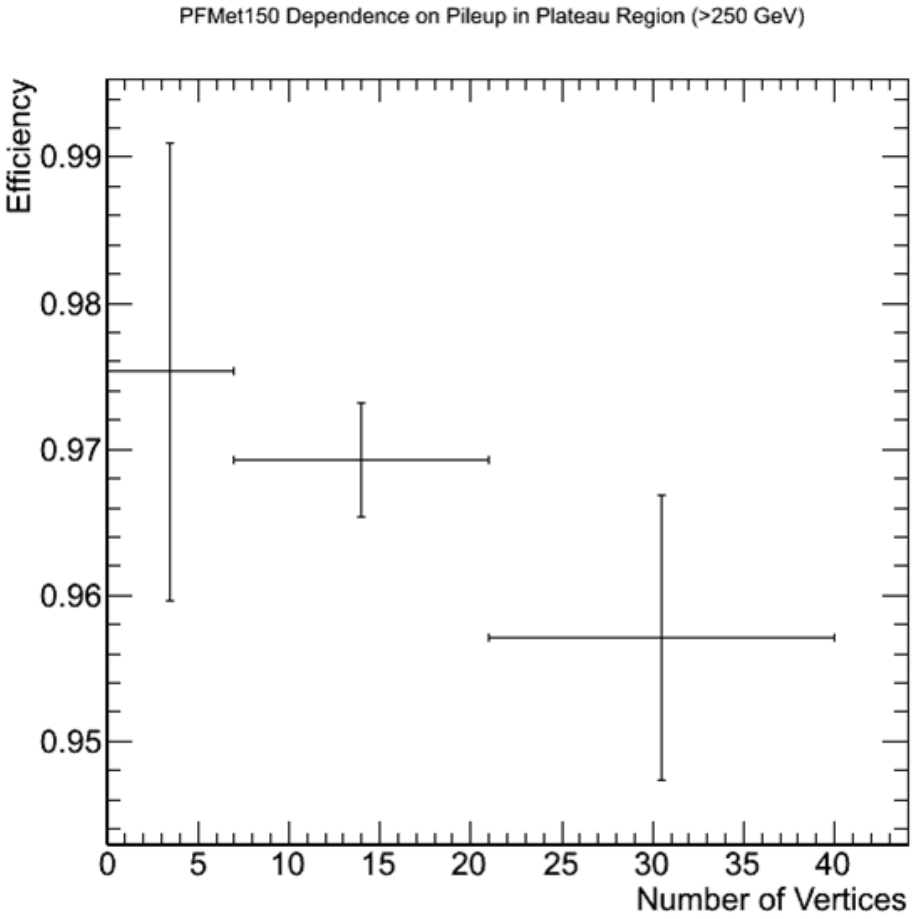

Fig. III.4. A simple measurement of the plateau efficiency using a linear fit in the region where MHT > 250. The parametrized values are shown in Table III.2 with a comparison to their value in III.1.

CHAPTER IV
CONCLUSIONS

MET Trigger Efficiency

In conclusion, we have studied the efficiency of the momentum imbalance trigger for use in searches for SUSY using the CMS detector at the LHC. This trigger allows the detector to select candidate events with large MET in real time from the millions of collisions that occur each second. We have shown that the trigger has a plateau efficiency that is of the order of 95% which makes it very useful for new physics searches. This plateau allows for sensitivity to new, heavy particles predicted by SUSY. In addition, we have studied the plateau efficiency as a function of the number of hard-scattering events that occurs in the detector. There is some evidence that the efficiency does fall for large number of pile-up events in the detector. While it is small for the data taking that was done, this dependence would cause difficulties for any analysis that uses this same trigger for any new data with high instantaneous luminosities and consider this trigger potentially less attractive for use in future studies.

Other studies are ongoing to see if the loss of efficiency at high MHT could be ameliorated or even removed by removing events that hit parts of the detector that may have caused mis-measurements. While important filters were used in the trigger codes to remove systematic errors in the calorimeters such as when an event crossed a bad crystal in the ECAL, there are some additional optional filters that could also be added to see if they cause an improvement to the efficiency or even reduce the effect of pile-up.

With the study of the efficiency of the trigger now complete and a clear indication that it is a powerful way to select candidate events in real time, we mention how it fits into the overall

search for SUSY in the coannihilation region, and future versions of this analysis with higher luminosity.

With a full set of data, we can now search the events for the presence of SUSY. The efficiency measurement allows us to work backwards to determine the sensitivity of any search and/or determine the number of SUSY events that were produced since we can estimate the fraction that were rejected by the trigger.

The set of events selected by the trigger can then be searched for the presence of two taus. This subset of events can be compared to expectations from SM sources as well as the predictions of SUSY. This important set of steps in the analysis falls outside the scope of this thesis, but is being completed by the analysis team at Texas A&M.

As we look forward towards future data taking, these studies can be useful to make future searches more powerful.

Future Prospects for SUSY Models

It is also worth commenting on future versions of this search from a motivation standpoint. When this analysis began, the coannihilation region was considered a best bet for discovery of dark matter. However, since then with the Higgs having recently been found at the LHC with a mass of 125 GeV, there are new limits for different physics models. Also, a previous search for the coannihilation region with 2011 data did not see any events [12]. Similarly, other searches for SUSY have turned up no hints for new physics, and measurements of rare decays have also put limits on deviations from SM predictions [13]. For these reasons, SUSY models where mSUGRA is the method of symmetry-breaking have fallen out of favor [14]. In the mean time, other models have come into favor that are similar to this search, but slightly different. These models also predict events with high MET. Since some of the properties of these events are different, other trigger approaches are being studied, but techniques used to

determine the efficiency of the momentum imbalance trigger can be used for them as well, allowing the value of this thesis work to be felt for many years.

REFERENCES

[1] Particle Data Group, S. Eidelman *et al.*, Phys. Lett. B **592** (2004) 1

[2] G. Aad *et al.* (ATLAS Collaboration), Phys. Lett. B **716**, (2012) 1; S. Chatrchyan *et al.* (CMS Collaboration), Phys. Lett. B **716** (2012) 30

[3] E. Komatsu, *et al.*, Astrophys. J. Suppl. Ser. **192** (2011) 18

[4] D.Z. Freedman, P. Van Niewenhuisen, and S. Ferrara, Phys. Rev. D **13** (1976) 3214

[5] S. Martin, arXiv:hep-ph/9709356

[6] S. Deser and B. Zumino, Phys. Lett. B **65** (1976) 369

[7] R. Arnowitt, B. Dutta, T. Kamon, N. Kolev, and D. Toback, Phys. Lett. B **639** (2006) 46

[8] R. Arnowitt, B. Dutta, A. Gurrola, T. Kamon, A. Krislock, and D. Toback, Phys. Rev. Lett. **100**, 231802 (2008)

[9] R. Arnowitt, A. Aurisano, B. Dutta, T. Kamon, N. Kolev, P. Simeon, D. Toback, and P. Wagner Phys. Lett. B **649** (2007) 73

[10] CMS Collaboration, http://cds.cern.ch/record/922757/files/lhcc-2006-001.pdf

[11] CMS Collaboration, doi:10.1088/0954-3899/6/S01

[12] R. Montalvo, Ph.D. Thesis (2013), http://roy.physics.tamu.edu/Thesis/Drafts/Thesis.pdf

[13] R. Aaij, *et al.* (LHCb Collaboration), Phys. Rev. Lett. 110, 021801 (2013)

[14] S. Akula, P. Nath, and G. Peim, Phys. Lett. B **717** (2012) 188